Forest Ecology and Management 354 (2015) 139–148

Contents lists available at ScienceDirect

Forest Ecology and Management

journal homepage: www.elsevier.com/locate/foreco

Carbon stocks of mangroves within the Zambezi River Delta, Mozambique

Christina E. Stringer [a,*], Carl C. Trettin [a], Stanley J. Zarnoch [b], Wenwu Tang [c,d]

[a] Center for Forested Wetlands Research, Southern Research Station, USDA Forest Service, Cordesville, SC, USA
[b] Forest Inventory and Analysis, Southern Research Station, USDA Forest Service, Clemson, SC, USA
[c] Department of Geography and Earth Sciences, University of North Carolina at Charlotte, Charlotte, NC, USA
[d] Center for Applied Geographic Information Science, University of North Carolina at Charlotte, Charlotte, NC, USA

ARTICLE INFO

Article history:
Received 9 April 2015
Received in revised form 18 June 2015
Accepted 20 June 2015
Available online 26 June 2015

Keywords:
Blue carbon
Carbon inventory
East Africa
Forested wetland

ABSTRACT

Mangroves are well-known for their numerous ecosystem services, including storing a globally significant C pool. There is increasing interest in the inclusion of mangroves in national climate change mitigation and adaptation plans in developing nations as they become involved with incentive programs for climate change mitigation. The quality and precision of data required by these programs necessitates the use of an inventory approach that allows for quantification, rather than general characterization, of C stocks. In this study, we quantified the ecosystem C stock of the Zambezi River Delta mangroves utilizing a rigorous, yet operationally feasible approach. We applied a stratified random sampling inventory design, based on five forest canopy height classes, derived from Ice, Cloud, and Land Elevation Satellite/Geoscience Laser Altimeter System (ICE Sat/GLAS) and the Shuttle Radar Topography Mission (SRTM) data, and a Spatial Decision Support System to allocate inventory plots. Carbon content in above- and below-ground biomass pools in addition to soils to a depth of 200 cm was measured. The average biomass C density for the height classes ranged from 99.2 Mg C ha^{-1} to 341.3 Mg C ha^{-1}. Soil C density was the largest measured C pool, containing 274.6 Mg C ha^{-1} to 314.1 Mg C ha^{-1} and accounting for 45–73% of the height class ecosystem C densities, which ranged from 373.8 Mg C ha^{-1} to 620.8 Mg C ha^{-1}. The ecosystem C density estimates for the five strata were weighted based on their spatial distribution across the landscape to yield a total C stock for the Zambezi River Delta mangroves of 1.4×10^7 Mg C. The error bounds from the 95% confidence interval are ±6% of our ecosystem C stock estimate, well within acceptable levels of uncertainty.

Published by Elsevier B.V.

1. Introduction

Mangroves are recognized for their numerous ecosystem services and functions that are critical to environmental health and human well-being. Although mangroves comprise only 0.7% of the world's tropical forest area (Giri et al., 2011), they have been shown to contain globally significant C pools, particularly in soils, storing up to three times more C per area than typical upland tropical forests (Donato et al., 2011; Kauffman et al., 2011). Studies from around the world have highlighted the capacity of mangroves to store C, revealing a wide range of ecosystem C stock estimations (Adame et al., 2013; Alongi, 2014; Jones et al., 2014; Rahman et al., 2014). The large amount of C processing that occurs in mangrove environments (Dittmar et al., 2006; Kristensen et al., 2008) is inextricably linked to the ecosystem services for which they are renowned, particularly sediment retention, fishery resources, and nutrient filtration (Alongi, 2002; Bouillon et al., 2008).

After fossil fuel combustion, deforestation and forest degradation constitute the second largest anthropogenic source of C dioxide to the atmosphere, comprising between 8% and 20% of total emissions (van der Werf et al., 2009; IPCC, 2013). International incentive programs for climate change mitigation are being considered as a viable option for reducing greenhouse-gas emissions from the land use sector. These programs include financial mechanisms regulated by compliance or voluntary C markets aimed to conserve or enhance ecosystem C stocks, thus reducing or avoiding emissions from land use and land cover change (Gullison et al., 2007). One mechanism that has been a focus of international climate policy is the UN's Reducing Emissions from Deforestation and Forest Degradation (REDD+) program, which proposes financial incentives to help developing countries reduce deforestation

* Corresponding author.
E-mail address: christinaestringer@fs.fed.us (C.E. Stringer).

http://dx.doi.org/10.1016/j.foreco.2015.06.027
0378-1127/Published by Elsevier B.V.

and degradation rates, build capacity for conservation and sustainable forest management, and enhance forest C stocks (UN-REDD, 2011). While the majority of the preparations have focused on terrestrial forests, the large C sequestration capacity of mangroves and high rates of mangrove deforestation worldwide have sparked considerable interest about including them in REDD+ programs.

Africa contains approximately 20% of the world's mangroves (Giri et al., 2011). Within Africa, Mozambique has the second largest area of mangrove cover after Nigeria (Fatoyinbo and Simard, 2013). Globally, Mozambique ranks 13th in mangrove coverage, equivalent to approximately 2.3% of the global mangrove forest area (Giri et al., 2011). While the functions of mangroves in Mozambique are analogous to those elsewhere (e.g., storm protection and fish nurseries), their associated goods and services are particularly valuable given the dependence of local communities on the forests and near-shore fisheries (Government of Mozambique, 2009).

The Zambezi River Delta mangrove extends for 180 km along the coast and approximately 50 km inland, accounting for almost 50% of the mangrove area in Mozambique and forming the second largest continuous mangrove habitat in Africa (Barbosa et al., 2001). The stature and importance of the Zambezi River Delta mangrove to the Mozambican people make it an area of interest for conservation and marketing of C sequestration potential and other ecosystem services.

Mangrove forests are often located in remote areas that are extremely difficult to access, making thorough investigations logistically challenging, as is the case with the Zambezi River Delta. Regardless of these inherent difficulties, the quality and precision of data required by programs like REDD+ necessitate the use of an inventory approach that allows for objective quantification, rather than general characterization, of the C stocks within the area of interest. The designed inventory provides the basis for quantifying C stocks, assessing uncertainties, and monitoring changes over time. The recent inventory of mangroves in Madagascar (Jones et al., 2014) is the only comprehensive C inventory performed to date in Africa, and one of just a few globally (Kauffman et al., 2011; Adame et al., 2013; Kauffman et al., 2014; Rahman et al., 2014). While approaches for forest inventory are well documented (e.g., Bechtold and Patterson, 2005), the challenge in mangroves is the design of an approach that provides a robust estimate of the C stock and is operationally efficient. Our objective was to quantify the mangrove C stock within the Zambezi River Delta that can serve as a baseline for measurement, reporting and verification (MRV).

2. Study area

The Zambezi River Delta (Fig. 1) comprises an area of approximately 12,000 km^2, extending 120 km downstream of the Zambezi and Shire Rivers confluence to the Indian Ocean. It also extends 200 km southwest–northeast along the coastline, from the Cuacua River, to the Zuni River Delta. The climate of the region is tropical, with a distinct dry winter season from April to October and a wet summer season from October to March (Barbosa et al., 2001; Hoguane, 2007). The mean annual precipitation ranges from 1000 mm at the most upstream regions of the delta to more than 1400 mm along the coast, with considerable inter-annual variation (Bento et al., 2007). Eighty-five percent of the rain falls from mid-November to late March (Tweddle, 2013). Mean monthly temperatures range from a minimum of 27 °C in June to a maximum of 37 °C in October (Tweddle, 2013).

The water levels in the Zambezi River Delta are reflective of the cumulative runoff patterns in the upstream sub-basins, with an estimated average water volume of 108×10^9 m^3 reaching the delta on an annual basis (Beilfuss and Santos, 2001). The tidal regime in the delta is semi-diurnal, with a spring tide maximum amplitude of 4.1 m (Beilfuss and Santos, 2001; Coleman, 2004). This tidal range is the largest in Mozambique and in the dry season tidal influence reaches 80 km upstream (Beilfuss and Santos, 2001).

The vegetation of the Zambezi River Delta is a mixture of woodlands, savanna, grasslands, mangroves, and coastal dunes within a mosaic of wetlands (Beilfuss et al., 2001). Small villages with accompanying subsistence agriculture plots are scattered throughout the extent of the delta. Mangrove communities occur on mud flats within the coastal estuary, occupying an area of approximately 30,267 ha, as delineated by Giri et al. (2011) (Fig. 1). These mud flats are composed of dark silt and clayey alluvium, rich in organic matter (Beilfuss et al., 2001). There are eight mangrove species present in the delta, representative of all species reported to occur in Mozambique: *Sonneratia alba* Smith, *Avicennia marina* (Forsskk.) Vierh., *Rhizophora mucronata* Lam., *Ceriops tagal* (Per.) C.B. Robinson, *Bruguiera gymnorrhiza* (L.) Lam., *Lumnitzera racemosa* Wild., *Heritiera littoralis* Alton, and *Xylocarpus granatum* Koenig. Mangrove associate species tend to occur in elevated areas with less tidal inundation (Vilankulos and Marquez, 2000) and include *Guettarda speciosa* L., *Hibiscus tiliaceous* L., and the large fern *Achrostichum aureum* L. (Barbosa et al., 2001; Beilfuss et al., 2001). Thickets of *Barringtonia racemosa* (L.) Spreng. also occur along the furthest upstream reaches of tidal influence within the estuary (Beilfuss et al., 2001).

The geomorphology of the delta is heavily affected by upstream activities and water flows, especially the operation of the Kariba and Cahora Bassa Dams. The dams have not only reduced fresh-water discharge to the delta, but also diminished sediment transport, resulting in coastal zone erosion and a reduction of sediment-maintained habitats, including mangroves (Davies et al., 2000). The degree to which these changes in flows and deposition directly affect the vegetative communities within the delta has not been well studied. Additionally, the delta is subject to frequent storms that cause geomorphic changes and can also directly damage mangrove stands (Beilfuss et al., 2001).

3. Methods

3.1. Inventory design

The inventory area included the entire 30,267 ha of mangrove forest, distributed along the north and south sides of the Zambezi River, as delineated by Giri et al. (2011). We used a stratified random sampling design, since stratification can improve the precision of the inventory (Cormack, 1988; Nusser et al., 1998). Mangrove canopy height, derived from Ice, Cloud, and Land Elevation Satellite/Geoscience Laser Altimeter System (ICE Sat/GLAS) and the Shuttle Radar Topography Mission (SRTM) data, is available for Africa (Fatoyinbo and Simard, 2013). We used the mangrove canopy height data as the basis for stratification, because forest height is functionally related to biomass estimation. Five canopy height classes were distinguished within the Zambezi River Delta using a Jenks natural breaks optimization: 2–6.9 m (HC1), 7–9.9 m (HC2), 10–12.9 m (HC3), 13–17.9 m (HC4), and 18–29 m (HC5). The number of plots per height stratum was determined by using a proportional allocation with respect to the total area in each stratum, based on the remote sensing mangrove coverage pixels.

The field work was conducted over two field seasons in September and October of 2012 and 2013. Our sampling approach used 7 m radius subplots (0.0154 ha) nested within a 0.52 ha square plot. The purpose of the subplots was to accommodate inherent spatial variation within the plot that was represented in

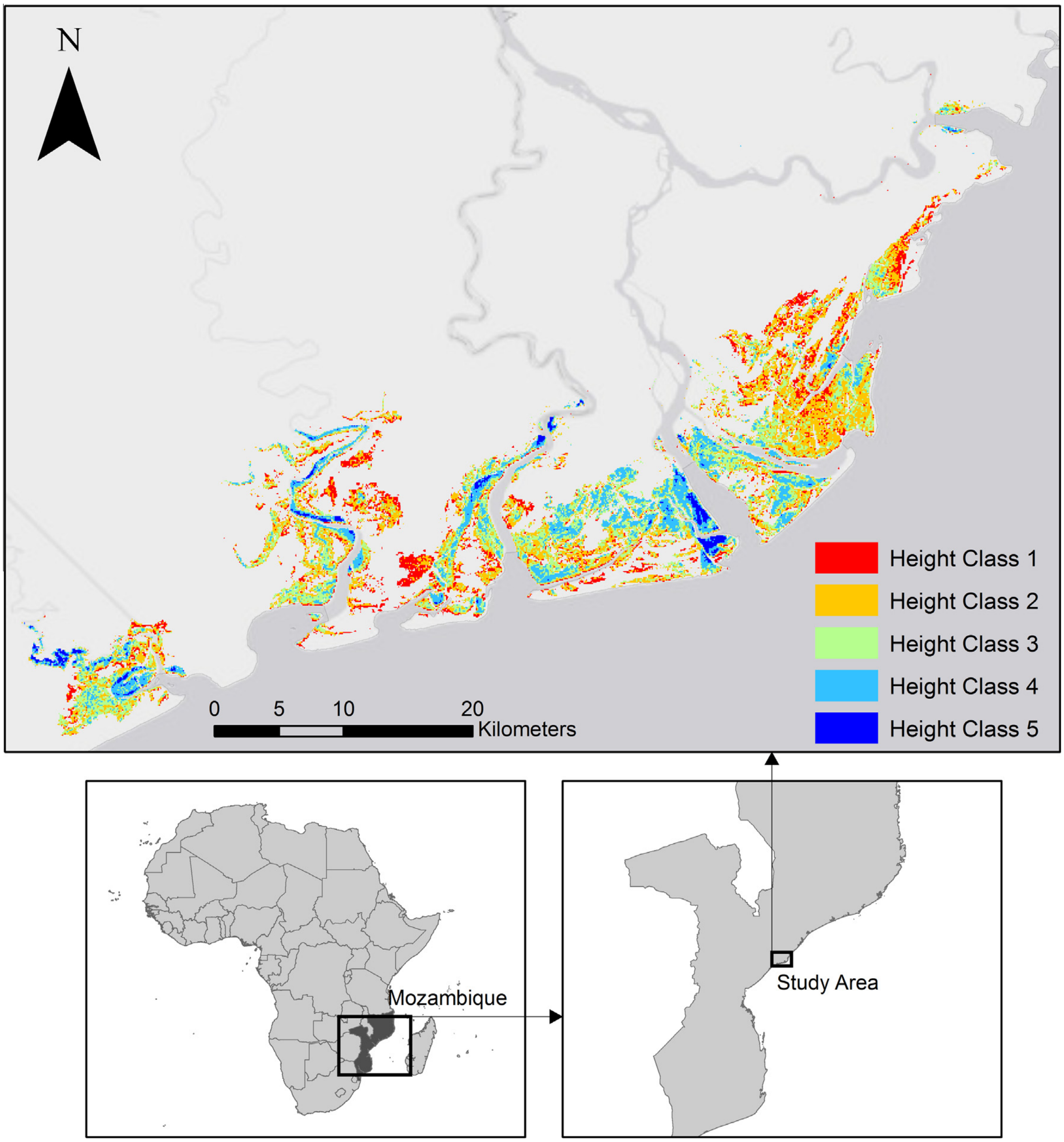

Fig. 1. The Zambezi River Delta study area and its position on the Mozambican coast. The mangrove extent considered in this inventory (Giri et al., 2011) is represented categorically by canopy height class classification (Fatoyinbo and Simard, 2013).

the mangrove stands. During the first season, 12 plots containing 6 subplots, were sampled. Analyses of the 2012 data demonstrated that the number of subplots could be reduced to 5 without a loss in precision, so the number of subplots sampled in 2013 was reduced to 5. We also used the 2012 tree basal area data to determine the total number of plots needed to complete the inventory in during the 2013 field mission. The appropriate sampling size, defined as having a mean with a confidence interval of ±20%, was determined to be 52 plots, using procedures outlined by Bartlett et al. (2001). Accordingly, 40 additional plots each with 5 subplots were sampled in 2013.

A Spatial Decision Support System (SDSS) (Densham, 1991) was used to locate plots within each stratum, providing randomization of plot selection and the ability to consider various logistical constraints including distance from camp locations and accessibility, as well as ensuring that each plot was located within uniform areas of the stratum, defined as minimum of four contiguous pixels (90 × 90 m) in a given height class.

3.2. Tree biomass

Diameter at breast height (DBH), height, and species were recorded for understory and overstory trees in each subplot. Overstory trees, defined by DBH > 5 cm, were measured within the 7 m subplots. All small understory trees and saplings (DBH < 5 cm) reaching at least 1.3 m (breast height) were measured in a 2 m radius subplot nested within the 7 m radius subplot. All diameters were measured to the nearest 0.1 cm using a diameter tape. If the tree was dead, a decay class of 1, 2, or 3, as defined by Kauffman and Donato (2012), was recorded in addition to the DBH. Some mangroves have root adaptations that affect the way in which diameter is measured; if a buttress stem was encountered, the diameter was measured at the point directly above the buttress. If a tree had prop roots (e.g., *R. mucronata*), measurements were made just above the highest prop root. Height was measured to the nearest 0.5 m for every tree using a hypsometer (Haglof Vertex III, Haglof Inc, Sweden).

Above-(B_{AG}, kg) and below-ground (B_{BG}, kg) biomass pools were determined for each live tree, both overstory and understory, using equations developed by Komiyama et al. (2005, 2008):

$$B_{AG} = 0.251\rho D^{2.46} \quad (1)$$

$$B_{BG} = 0.199\rho^{0.899} D^{2.22} \quad (2)$$

where ρ represents wood density (g cm^{-3}) and D denotes DBH (cm). General equations were selected since local or regional species-specific allometric equations have not been developed for all species occurring within the study area. While it has been shown that these general equations can produce much larger estimates of biomass than species-specific equations, these differences are slight for trees with DBH < 20 cm (Kauffman and Donato, 2012), which describes 92% of the overstory trees sampled in this inventory. Species-specific ρ values were employed, using the mid-value of the published density range for each species (World Agroforestry Center, 2013). For any tree encountered where the species was unknown, we used the average ρ among all species present, 0.86 g cm^{-3}.

Above- and below-ground biomass estimates for standing dead trees were conditional on decay class. For the above-ground biomass for decay classes 1 and 2, the same allometric equation used for live trees was applied to each standing dead tree, using a density of 0.69 g cm^{-3}, as species and wood density were not recorded for dead trees, and it has been considered a reasonable estimate of large solid downed wood (Kauffman and Donato, 2012). These estimates were adjusted for the loss of leaves and branches by subtracting 2.5% and 15% of the biomass for classes 1 and 2, respectively (Kauffman and Donato, 2012). The above-ground biomass for class 3 standing dead trees was determined by applying the formula of the volume of a cone. Once volume was determined, the value was multiplied by wood density (0.69 g cm^{-3}) to determine biomass.

Below-ground biomass for all classes of standing dead trees was determined using the same equation used for the live trees. Consideration was made for the swift loss of fine roots once a tree dies. Because of previous reports of mangroves supporting a large proportion of fine root biomass—as much as 66% of total below-ground biomass for some species (Komiyama et al., 1987)—we corrected our estimates by subtracting 46%, a conservative estimate still within the ranges reported by other studies (Komiyama et al., 1987, 2000).

The calculated individual standing tree biomass values, both live and dead, were summed at the subplot level and normalized for the subplot area to provide a total subplot biomass density (Mg ha^{-1}). Biomass density estimates were converted to C mass by using concentration factors of 0.50 and 0.39 for above-ground and below-ground estimates, respectively (Kauffman and Donato, 2012).

3.3. Downed woody debris

Downed woody debris, dead wood laying on the forest floor, was measured using the planar intersect technique, which involves counting the number of intersections of debris pieces along a transect (Van Wagner, 1968; Brown, 1971). Four 12 m long transects were established in each subplot. Downed, dead, wood material was classified into four size classes based on diameter: fine (0–0.6 cm), small (0.6–2.5 cm), medium (2.5–7.6 cm), and large (>7.6 cm). In each of the three smaller size classes, the number of transect intersections was tallied along a designated portion of the transect. The individual diameter and state of decay (solid or rotten) were recorded for each large wood piece (>7.6 cm) along the full length of the transect.

Downed woody debris biomass estimates were made by first determining the volume of each size class through the use of scaling equations (Van Wagner, 1968; Brown, 1971) using the mean diameter of the range for each of the 3 smaller size classes. The volume of each size class was converted to biomass by multiplying by wood density, using the estimates of Kauffman and Donato (2012). The biomass estimates were converted to C mass by using a concentration of 0.50, as recommended by Kauffman and Donato (2012).

3.4. Litter and ground Vegetation

Two 50 cm $\times$ 50 cm quadrats were established at both the 6 m and 12 m points of each of the 4 subplot transects to collect all litter, except downed woody debris, down to the mineral soil surface. Two 50 cm $\times$ 50 cm quadrats were established at the 10 m transect point of each of the 4 subplot transects to harvest all ground vegetation < 1.3 m in height. Ground vegetation included any sort of seed, seedling, propagule, or pneumatophore present in the quadrats. Each of these sample types was composited for each subplot and then weighed in the field to the nearest gram. To determine water content, representative subsamples from each plot were weighed in the lab and then placed in a 60 °C drying oven and dried until a constant weight was achieved. This wet to dry mass ratio was used to adjust the masses of the whole litter and ground vegetation samples to a dry-weight basis, which were then scaled to a per-hectare estimate. Mass was converted to C concentration by applying a conversion factor of 0.45, as recommended by Kauffman and Donato (2012).

3.5. Soils

The soil was sampled to a depth of 200 cm from a point near the center of each subplot using a stainless steel gouge auger with a semi-cylindrical chamber 1 m long and 18.8 cm^2 in cross-sectional area (AMS Inc, American Falls, Idaho, USA). The gouge auger facilitated collecting undisturbed volumetric soil samples at 6 intervals: 5–10 cm, 20–25 cm, 35–40 cm, 70–75 cm, 145–150 cm, and 190–195 cm. These intervals represented the soil depths of: 0–15 cm, 15–30 cm, 30–45 cm, 45–110 cm, 110–185 cm, and 185–200 cm, respectively. At each sampling interval, a 5 cm section of the soil core, measured to the nearest mm, was obtained. The samples were returned to a laboratory and dried at 60 °C until a constant weight was achieved. To determine the air-dry to oven-dry ratio, a subset of 50 samples was dried at 105 °C until a constant weight was achieved. The air-dried to oven-dried ratio was calculated for each of these samples and the average (1.01 ± 0.003) applied to the air-dried mass of all soil samples to adjust the mass to an oven-dried basis. The bulk density (g cm^{-3}) of each sample was calculated by dividing the oven-dried mass by the volume of the sample. Prior to further analysis, a subset of 100 soil samples was tested for the presence of carbonates following standard procedures (Thomas, 1996); none tested positive.

Subsamples of each soil sample were pulverized using a high-energy ball mill (SPEX SamplePrep, Metuchen, NJ, USA) prior to C concentration determination using a Perkin Elmer 2400 Series II CHNS/O Analyzer (Perkin Elmer, Waltham, MA, USA). Instrument settings and procedures followed the recommended application protocols described by Perkin Elmer (2010). Duplicates were analyzed for quality assurance (duplicate samples were ±0.1% C or better) and certified standards were used for calibration.

Soil sample C density was determined as

$$C_S^n = D_b\, d\, C \quad (3)$$

where C_S^n is the soil C density (Mg ha^{-1}) for interval n (n = 1, 2,. . .,6), D_b is the bulk density (g cm^{-3}), d is the length of the depth interval (cm), and C is the sample C concentration, expressed as a percent. The C density of each interval, C_S^n was summed to determine the total soil C density, C_s, for each core.

3.6. Ecosystem carbon stock

The ecosystem C density (Mg ha^{-1}) for each height class was estimated by summing the C density values for each of the component pools:

$$\text{Ecosystem C} = C_{O-AGB} + C_{O-BGB} + C_{U-AGB} + C_{U-BGB} + C_{D-AGB} + C_{D-BGB} + C_L + C_{GV} + C_{WD} + C_S \quad (4)$$

where each term is the C density (Mg ha^{-1}) for each component: C_{O-AGB} and C_{O-BGB} are overstory above-ground and below-ground biomass, respectively; C_{U-AGB} and C_{U-BGB} are understory above-ground and below-ground biomass, respectively; C_{D-AGB} and C_{D-BGB} are standing dead tree above-ground and below-ground biomass, respectively; C_L is litter; C_{GV} is ground vegetation; C_{WD} is downed woody debris; and C_S is soils.

Once a per-hectare estimate was obtained for each height class, the ecosystem C stock was estimated by multiplying each of the height class total C densities by their respective areas and summing them to arrive at a final C mass (Mg).

3.7. Inventory and statistical analyses

The inventory sampling design consisted of a stratified random sample with five height class strata. Within each stratum a random sample of plots was selected. Sample means, along with variances and 95% confidence intervals, were computed for each stratum using PROC SURVEYMEANS (SAS Inc., 2011), with plots defined as clusters of either 5 or 6 subplots and where the finite population correction was ignored because the sampling fraction was very low. Since this study was designed as an inventory, traditional sample survey methodology (Cochran, 1977) was used for all analyses instead of analysis of variance methodology which is more appropriate for experimental design studies. Thus, differences between height class means were performed with individual Satterthwaite two-sample *t*-tests (PROC TTEST) which allows for unequal variances for the two samples. All two-sample *t*-tests were performed at the 0.05 Type I error rate to illustrate differences between height classes. It must be realized that this error rate is on a comparison basis and does not provide the typical experimentwise error rate that is used for a set of multiple comparisons, such as Tukey's, between treatments in experimental design studies. If such an experimentwise error rate is desired, it could easily be accomplished by applying the Bonferroni approach which will provide an experimentwise error rate of 0.05 by adjusting the individual comparison 0.05 error rate to a lower value depending on the number of comparisons performed. The authors have all *p*-values from the Satterthwaite two-sample *t*-tests and these could easily be used to perform Bonferroni adjusted multiple comparisons if an experimentwise 0.05 error rate is desired (available upon request). Individual stratum totals were obtained by multiplying each stratum mean by its area. Overall means for the Zambezi River Delta were computed as the sum of weighted strata means where the weights were the proportion of the total area in each stratum. Similarly, total mangrove C storage for the Delta was determined as the overall mean times the total area. Since the areas were known constants, variances for means and totals were computed in the typical manner by squaring the weights, multiplying by the variances, and summing accordingly (Cochran, 1977).

4. Results

4.1. Carbon stocks: biomass

The full range of mangrove species present in the Zambezi River Delta was distributed heterogeneously throughout the inventory area, with no consistent patterns in species abundance within or among height strata. The contribution of each mangrove species to above-ground biomass varied within each height class, with no clear patterns or trends exhibited (Fig. 2). The most pronounced dominance occurred in HC1, where *X. granatum* and *A. marina* contributed 39% and 38%, respectively, to the total biomass. *Laguncularia racemosa* was the least abundant species and consistently contributed the least amount of C to each HC. *Laguncularia racemosa* was not present in the overstory in HC2 and HC4, and accounted for only 2% of aboveground tree C in HC5.

Overstory biomass was the dominant above-ground C pool, with densities increasing from 55.4 Mg C ha^{-1} in HC1 to 241.3 Mg C ha^{-1} in HC5 (Table 1), and accounting for as much as 89% of the total above-ground biomass C stock in the two upper height classes. Overstory biomass was significantly different among canopy height classes. The mean understory C density ranged from 3.0 Mg ha^{-1} to 11.0 Mg ha^{-1}, with no significant

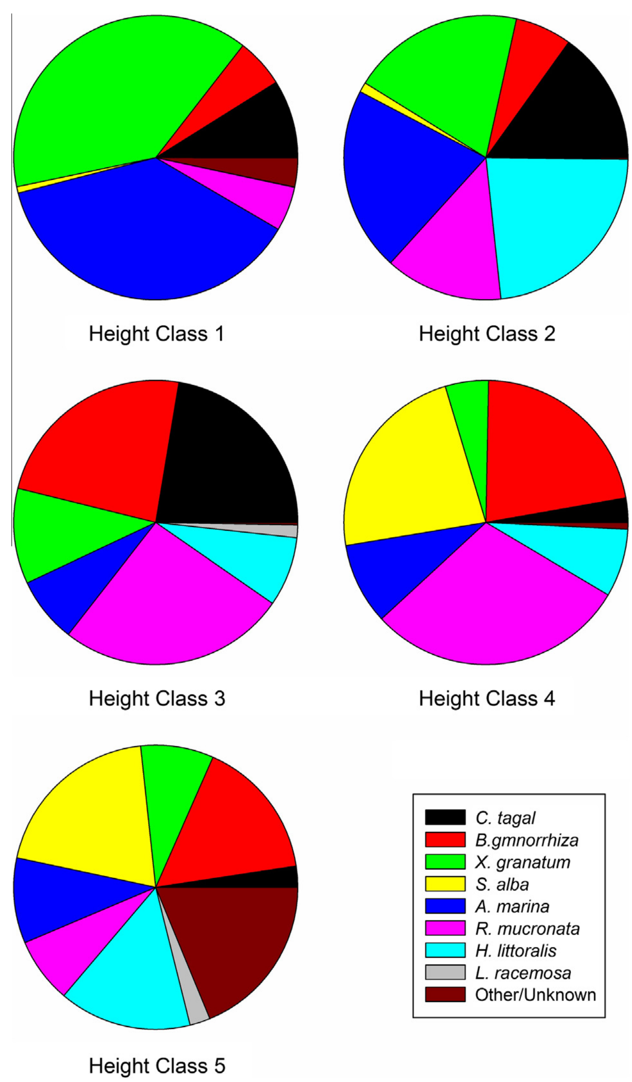

Fig. 2. Proportional contribution of each mangrove species to total above-ground biomass for overstory trees in each of the 5 height classes.

Table 1
Carbon density, mean (standard error), for biomass and soil pools within each height class, and the corresponding ecosystem C stock. Within each row, means followed by the same letter are not significantly different at $p = 0.05$, based on individual two-sample t-tests.

	Carbon density (Mg C ha^{-1})									
	Height Class 1		Height Class 2		Height Class 3		Height Class 4		Height Class 5	
Above-ground biomass										
Overstory	55.4^{a}	(11.8)	96.7^{ab}	(16.4)	127.4^{bc}	(20.2)	183.3^{cd}	(20.6)	241.3^{d}	(36.2)
Understory	7.7^{a}	(3.7)	7.4^{a}	(2.3)	11.0^{a}	(5.7)	3.7^{a}	(1.3)	3.0^{a}	(1.4)
Ground vegetation	0.1^{a}	(0.1)	0.0^{a}	(0.0)	0.1^{a}	(0.1)	0.2^{a}	(0.2)	0.0^{a}	(0.0)
Downed woody debris	6.7^{a}	(3.8)	7.8^{a}	(1.2)	6.8^{a}	(1.1)	9.2^{a}	(1.9)	12.5^{a}	(3.8)
Litter	0.2^{a}	(0.1)	0.3^{a}	(0.2)	0.3^{a}	(0.2)	0.4^{a}	(0.1)	0.7^{a}	(0.2)
Standing dead trees	5.4^{a}	(3.7)	3.7^{a}	1.0)	6.9^{a}	(1.3)	9.2^{a}	(3.1)	11.0^{a}	(4.9)
Total AGB	75.4^{a}	(12.6)	115.9^{ab}	(16.8)	152.5^{bc}	(17.7)	206.0^{cd}	(20.5)	268.5^{d}	(36.6)
Below-ground biomass										
Overstory	18.9^{a}	(3.8)	31.7^{ab}	(5.0)	40.4^{bc}	(5.9)	56.3^{cd}	(5.5)	69.7^{d}	(9.4)
Understory	3.6^{a}	(1.8)	3.4^{a}	(1.0)	5.0^{a}	(2.6)	1.7^{a}	(0.6)	1.4^{a}	(0.7)
Standing dead trees	1.3^{a}	(0.9)	0.9^{a}	(0.2)	1.5^{a}	(0.3)	1.7^{a}	(0.5)	1.7^{a}	(0.8)
Total BGB	23.8^{a}	(3.1)	36.0^{ab}	(5.0)	46.9^{bc}	(5.1)	59.7^{cd}	(5.2)	72.8^{d}	(9.4)
Soils	274.6^{a}	(25.0)	282.2^{a}	(11.2)	314.1^{a}	(14.8)	279.8^{a}	(13.6)	279.6^{a}	(17.6)
Total	373.8^{a}	(29.5)	434.1^{a}	(24.5)	513.5^{b}	(27.1)	545.5^{b}	(29.0)	620.8^{b}	(49.0)

differences amongst height classes (Table 1). Understory trees accounted for 1–10% of the total above-ground biomass C density.

The ground vegetation was a small component, containing less than 1% of the C measured in the above-ground biomass (Table 1). Height class means of ground vegetation ranged from a few kilograms to 0.2 Mg ha^{-1}, with no statistically-significant differences amongst height classes. The mean C density of downed woody debris ranged from 6.7 Mg ha^{-1} for HC1 to 12.5 Mg ha^{-1} for HC5, with no significant differences between height class means (Table 1). Downed woody debris was observed in each plot. The litter C density plot values ranged from 0 to 6.0 Mg ha^{-1} and height class means ranged from 0.2 Mg ha^{-1} for HC1, to 0.7 Mg ha^{-1} for HC5, with no significant differences amongst height classes (Table 1). Litter contributions to the C pool were low, with 46% of plots containing less than 1 Mg C ha^{-1}, and 19% containing no litter. Standing dead tree mean C density ranged from 3.7 Mg ha^{-1} for HC2, to 11.0 Mg ha^{-1} for HC5 with no significant differences (Table 1). Standing dead trees accounted for 8% of all overstory trees occurring within the delta.

Overstory, understory, and standing dead trees contributed to the below-ground biomass C stocks (e.g., roots). Mirroring the pattern of the above-ground biomass stocks, the overstory below-ground biomass mean C density increased with height class from 18.9 Mg ha^{-1} to 69.7 Mg ha^{-1} (Table 1). There were statistically-significant differences exhibited between all non-adjacent height classes. The ratio of overstory below-ground to above-ground biomass ranged from 0.32 for HC1 to 0.27 for HC5. The understory below-ground biomass C density means ranged from 1.4 Mg ha^{-1} for HC5, to 5.0 Mg ha^{-1} for HC3, with no significant differences amongst height classes (Table 1). The standing dead tree below-ground biomass C density means ranged from 0.9 Mg ha^{-1} for HC2, to 1.7 Mg ha^{-1} for both HC4 and 5, with no significant differences exhibited between any height classes.

4.2. Carbon stocks: soils

Soil characteristics were generally homogeneous throughout the study area. The mean soil bulk density, both within each height class (Table 2) and averaged among all the height classes for each interval (Fig. 3A), ranged from 0.7 to 0.9 g cm^{-3}, with no statistically significant differences with depth. Bulk density means for each sampling depth showed only a few significant differences among height classes in the three intervals sampled in the upper 45 cm, where the 0–15 cm in HC1 was significantly greater than those in the 110–185 or 185–200 cm (Table 2). The soil bulk density means within 45–110, 110–185, 185–200 cm were consistent across height classes, showing no statistically significant differences.

There was very little difference in soil C concentration within the sampled depth and among the height classes (Table 2). Carbon concentration tended to be the highest in the 0–15 cm interval for each height class, with the mean C concentration for the 0–15 cm soil greater in HC1 (1.7%) than HC5 (2.4%). The 30–45 cm soil depth was then only other interval where C concentration varied among height classes. The interval mean C concentration decreased with depth, with the exception of interval 2; interval 1 had a mean of 2.1%, decreasing to 1.6% at interval 6 (Fig. 3B). Despite this relatively narrow range in concentration, the variability within each sampling interval was very low, resulting in several statistically significant differences with depth. The overall mean C concentration in 0–15 cm was significantly greater than at the 110–185 and 185–200 cm soil depths. The soil at 185–200 cm contained significantly less C than the upper 0–110 cm of soil.

The mean soil C density ranged from 0.016 g cm^{-3} at 0–15 cm to 0.013 g cm^{-3} at within 185–200 cm, with the 4 intermediate intervals all having a mean of 0.014 g cm^{-3} (Fig. 3C). The mean C densities of the 0–15 and 185–200 soil depths were significantly different from each other, as well as the other 4 sampled intervals.

While there were several significant differences exhibited in both bulk density and C concentration in the shallower sampling intervals amongst height classes, when those components are multiplied and integrated over the sampling interval depth, the resulting interval C density means were consistent, showing no statistically significant differences between height classes (Table 2). The soil C density to a depth of 200 cm ranged from 274.6 Mg ha^{-1} for HC1, to 314.1 Mg ha^{-1} for HC3, with no statistically significant differences amongst height classes (Table 1).

4.3. Ecosystem carbon stock

The total C density, the combination of biomass and soils, ranged from 373.8 Mg ha^{-1} for HC1, to 620.8 Mg ha^{-1} for HC5 (Table 1). HC1 and HC2, while not significantly different from each other, were significantly different from the other 3 height classes. Total C density was not significantly different in HC3, HC4 and HC5. The soil component constituted the largest proportion of the total C density, comprising 45–73% of the total pool. The proportion of soil C was greater in the smaller height classes, where the above-ground vegetation contributed less C to the total stock

Table 2
Soil bulk density, C concentration, and C density means (standard errors) for each sampling interval within height classes. Within each row, means followed by the same letter are not significantly different at $p = 0.05$, based on individual two-sample t-tests.

	Soil depth (cm)	Height Class 1		Height Class 2		Height Class 3		Height Class 4		Height Class 5	
Bulk density (g cm^{-3})	0–15	0.94^{a}	(0.06)	0.81^{ab}	(0.04)	0.77^{ab}	(0.05)	0.74^{b}	(0.06)	0.77^{b}	(0.05)
	15–30	0.93^{a}	(0.06)	0.84^{a}	(0.04)	0.78^{ab}	(0.04)	0.77^{b}	(0.04)	0.78^{ab}	(0.05)
	30–45	0.95^{a}	(0.05)	0.83^{ab}	(0.05)	0.79^{b}	(0.05)	0.72^{b}	(0.05)	0.81^{ab}	(0.04)
	45–110	0.92^{a}	(0.08)	0.80^{a}	(0.04)	0.78^{a}	(0.03)	0.73^{a}	(0.04)	0.79^{a}	(0.04)
	110–185	0.85^{a}	(0.03)	0.88^{a}	(0.04)	0.83^{a}	(0.03)	0.81^{a}	(0.05)	0.89^{a}	(0.06)
	185–200	0.84^{a}	(0.02)	0.90^{a}	(0.04)	0.83^{a}	(0.05)	0.80^{a}	(0.05)	0.92^{a}	(0.10)
%C	0–15	1.74^{a}	(0.18)	2.01^{ab}	(0.14)	2.25^{ab}	(0.18)	2.28^{ab}	(0.20)	2.36^{b}	(0.19)
	15–30	1.59^{a}	(0.15)	1.69^{a}	(0.11)	2.03^{a}	(0.19)	1.89^{a}	(0.14)	1.94^{a}	(0.11)
	30–45	1.53^{a}	(0.11)	1.81^{ab}	(0.16)	2.11^{b}	(0.22)	2.12^{b}	(0.18)	1.94^{ab}	(0.15)
	45–110	1.49^{a}	(0.22)	1.93^{a}	(0.17)	2.07^{a}	(0.12)	1.99^{a}	(0.14)	1.75^{a}	(0.12)
	110–185	1.73^{a}	(0.20)	1.69^{a}	(0.09)	1.84^{a}	(0.13)	1.73^{a}	(0.10)	1.63^{a}	(0.22)
	185–200	1.56^{a}	(0.11)	1.45^{a}	(0.08)	1.73^{a}	(0.17)	1.63^{a}	(0.10)	1.50^{a}	(0.32)
Carbon density (Mg C ha^{-1})	0–15	23.44^{a}	(1.47)	23.40^{a}	(1.27)	24.33^{a}	(1.11)	24.08^{a}	(1.11)	26.66^{a}	(2.05)
	15–30	21.49^{a}	(1.14)	20.24^{a}	(0.86)	22.16^{a}	(1.09)	19.46^{a}	(0.89)	22.42^{a}	(1.45)
	30–45	21.07^{a}	(1.79)	20.71^{a}	(0.95)	22.99^{a}	(1.36)	21.67^{a}	(1.07)	22.68^{a}	(1.20)
	45–110	83.53^{a}	(7.70)	94.59^{a}	(5.72)	100.15^{a}	(3.67)	90.66^{a}	(4.58)	88.58^{a}	(5.45)
	110–185	110.00^{a}	(12.33)	108.02^{a}	(4.31)	110.07^{a}	(7.14)	101.61^{a}	(4.46)	101.43^{a}	(7.21)
	185–200	19.23^{a}	(1.34)	18.76^{a}	(0.82)	20.09^{a}	(1.55)	18.92^{a}	(1.20)	18.93^{a}	(2.92)

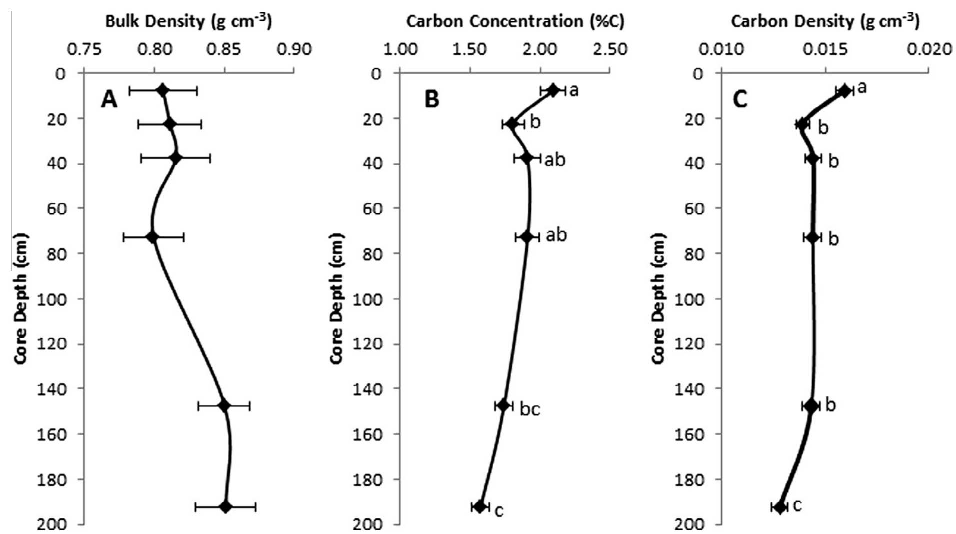

Fig. 3. Mean soil bulk density (A), C concentration (B), and C density (C) with depth; error bars represent the standard error of each mean. There were no statistically significant differences in soil bulk density means ($p > 0.05$). Carbon concentrations and densities followed by the same letter are not significantly different at $p = 0.05$, based on individual two-sample t-tests.

compared to the 2 tallest height categories. Differences in total C stocks across height classes were due to differences in overstory biomass pools, since soil C accounted for the majority of the ecosystem C and was not significantly different among height classes. The ecosystem C stock for the Zambezi River Delta was 1.4×10^7 Mg, with a standard error of 4.1×10^5 Mg and 95% confidence interval equivalent to $\pm 8.2 \times 10^5$ Mg of the overall mean (Table 3).

Table 3
Total C mass, mean (standard error), calculated for each height class and resulting ecosystem C stock estimate for the Zambezi River Delta.

Height class	Total carbon stock (Mg C ha^{-1})		Area (ha)	Total carbon (Mg $*$ 10^{6})	
1	373.8	(29.5)	4730	1.8	(0.1)
2	434.1	(24.5)	10,536	4.6	(0.3)
3	513.5	(27.1)	8610	4.4	(0.2)
4	545.5	(29.0)	5522	3.0	(0.2)
5	620.8	(49.0)	869	0.5	(0.04)
Total			30,267	14.3	(0.4)

5. Discussion

5.1. Ecosystem carbon stock

Our estimate of mean ecosystem C storage of Zambezi River Delta mangroves (484 Mg C ha^{-1}) is within the wide range of values reported in recent studies (Adame et al., 2013; Jones et al., 2014; Rahman et al., 2014), but lower than the mean presented in a recent synthesis by Alongi (2012) (Fig. 4A). The highest mean estimate was 937 Mg C ha^{-1}, derived from a synthesis of regional data for Indo-Pacific mangroves (Alongi, 2012). A large-scale mangrove inventory in the Bangladesh Sundarbans reported lower C densities, with means ranging from 159 Mg C ha^{-1} to 360 Mg C ha^{-1} (Rahman et al., 2014). A study in Madagascar, the only other inventory performed in the west Indian Ocean region, conveyed a similar C density to the Zambezi, with a mean of 457 Mg C ha^{-1} (Jones et al., 2014). Even estimates from equivalent mangrove species in the same geographical region can illustrate wide variation, as is the case in the Caribbean, where an investigation in Mexico reported a mean C density of 663 Mg C ha^{-1} (Adame

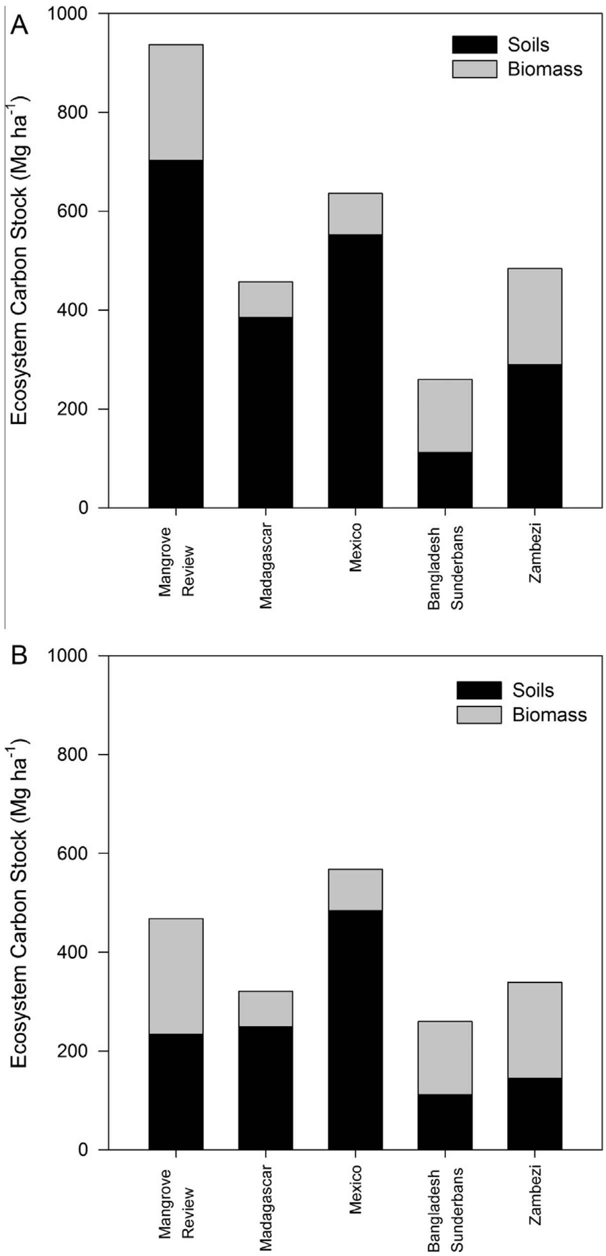

Fig. 4. Ecosystem carbon density estimates reported in mangrove C stock studies (A) and those same C density estimates normalized to include C from only the top 1 m of soil (B). Mangrove review data from Alongi (2012). Madagascar data from Jones et al. (2014). Mexico data from Adame et al. (2013). Bangladesh Sundarbans data (value shown is midpoint of range reported) from Rahman et al. (2014). Zambezi data from this study.

et al., 2013) and a study in the Dominican Republic provided a mean estimate of 853 Mg C ha^{-1} (Kauffman et al., 2014). This within-forest variation is most likely due to differences in productivity, which can result from variation in tree age, species composition, climate, geomorphology, and tidal influences (Bouillon et al., 2008; Alongi, 2014).

The wide range in estimates is due not only to actual differences in ecosystem structure, C storage capacity and hydrogeologic setting, but also to differences in sampling approaches and reporting (e.g., sampling design and intensity, availability of localized allometric equations). One of the largest differences in sampling and data reporting is the depth of soils considered, which ranges from ⩾3 m (Donato et al., 2011) to 1 m (Rahman et al., 2014). Since soil C density is often very high for mangrove ecosystems, this difference has a large influence on estimates of total ecosystem C. When the entire soil C stock as reported in each inventory is considered, the contribution of soils to ecosystem C stock ranged from 43% in the Bangladesh Sundarbans (Rahman et al., 2014) to 87% in Mexico (Adame et al., 2013) (Fig. 4A). This study fell in the middle of that range, with soil C composing 60% of the ecosystem C stock. Normalizing soil C stocks to the upper 1 m layer reduces the range of mangrove C storage reported across studies and is necessary for an effective inter-study comparison (Fig. 4B). With the exception of one study presented, 1 m deep soil C densities are similar to the default IPCC values for mangroves, which range from 471 Mg C ha^{-1} for organic soils to 286 Mg C ha^{-1} for mineral soils (IPCC, 2013).

5.2. Soil characteristics

The principal factors affecting the determination of soil C stocks are C concentration, bulk density, and the total depth over which the estimates are integrated. The global median soil C content of mangroves is 2.2% (Kristensen et al., 2008), which is similar to the means determined for the Zambezi River Delta (1.8%) and Madagascar (3.4%) (Jones et al., 2014). The same review illustrated that 44% of the available literature data showed C concentrations less than 2%, and 28% of reported values are between 2% and 5% (Kristensen et al., 2008). These results suggest that the C concentrations in the Zambezi, as well as Madagascar, are in the same range as 72% of the published data. In contrast, several recent studies which characterize ecosystem C stocks in mangroves report soil C concentrations ranging from 9% to 26% (Kauffman et al., 2011; Donato et al., 2012; Wang et al., 2013; Kauffman et al., 2014).

Mangrove soil bulk density has not been synthesized across the literature and is sometimes not directly discussed in C stock studies. Previous studies report mean bulk density values ranging from 0.18 g cm^{-3} (Kauffman et al., 2011) to 1.26 g cm^{-3} (Jones et al., 2014). Soil C density (g C cm^{-3}) is a metric that integrates C content and bulk density, and was shown by Chmura et al. (2003) to range from 0.023 to 0.114 g C cm^{-3} for mangrove soils. The mean C content for this study was below this, with depth interval means ranging from 0.013 g C cm^{-3} to 0.016 g C cm^{-3}, and also below the densities reported in Madagascar, which had a mean of 0.026 g C cm^{-3} (Jones et al., 2014). Soil C density can be a useful criterion to facilitate inter-study comparisons. However, the metric can also obscure differences in soil characteristics, as extremes in the two input parameters that determine C density can often counterbalance each other to produce similar values. Accordingly, thorough reporting of bulk density and C concentrations are critical to accurately evaluate any exhibited variability in soil character throughout a study area.

The lower bulk density and higher C concentration values often reported in mangrove studies are indicative of organic-rich soils and peats, while the mangrove sites characterized by higher bulk densities and lower C concentrations are reflective of a mineral soil substrate. The fact that mangroves exist in a wide range of soil types, even potentially within a single study area, contributes to the large variability in reported soil C stocks, and is an excellent example of why a well-defined inventory approach for assessing ecosystem C stocks is necessary to better account for the heterogeneity.

5.3. Variability of stock estimates

The above-ground biomass component of mangrove ecosystem C stocks is another source of variability in whole ecosystem C stock estimates. Several of the components that compose the biomass C pool, however, generally exhibit low variability within a study, and differ little between studies, reflecting general trends in mangrove ecosystem structure. Ground vegetation and litter contributions to the ecosystem C stock were insignificant in the Zambezi and did not vary significantly among height classes, corroborating reports from other studies that suggest the ground vegetation layer is generally negligible (Janzen, 1985) and is why it is frequently not sampled (e.g., (Donato et al., 2012). Similarly, the wood debris C component was uniform across the delta and within the range of means reported in other studies, which are generally between 10% and 15% of the total above-ground biomass (Kauffman et al., 2011; Donato et al., 2012; Adame et al., 2013; Kauffman et al., 2014).

Above-ground biomass C storage is dominated by overstory trees, and estimates can vary considerably depending on the mangrove forest structure and composition, as well as the sampling design employed. For Gazi Bay, a well-studied mangrove area in Kenya, Slim et al. (1996) and Kirui (2006) produced estimates of 125 Mg C ha^{-1} and 226 Mg C ha^{-1}, respectively, for *Rhizophora* species. More recently, Cohen et al. (2013) provided an estimate of 67 Mg C ha^{-1} for the same area, painting a very different picture about existing biomass. In Mexico, the above-ground tree biomass varied by approximately 60-fold between dwarf and tall mangrove vegetative classes (Adame et al., 2013). The variances exhibited in estimates at large spatial scales are most likely indicative of differences in forest composition, climatic conditions, hydrology, geomorphology, successional stage and history of disturbances (Fromard et al., 1998; Cohen et al., 2013).

Patterns in below-ground biomass are generally analogous to any trends exhibited in the above-ground biomass, owing to the use of DBH as the determinant for both calculations. The ratios of BGB to AGB in the Zambezi reflected the parameterization of the allometric equations, but is within the wide range of ratios (0.3–0.8) reported for other global mangroves (Komiyama et al., 2008; Kauffman and Donato, 2012). While the majority of studies utilize the same BGB allometric equation introduced by Komiyama et al. (2005), they also use appropriate, regionally-specific allometric equations for AGB, which most likely result in the wide range of calculated ratios. Mangrove root biomass characterization suffers from well-known difficulties in field measurements and in developing appropriate allometric equations (Kauffman et al., 2011). These issues mean that differences exhibited in both the below-ground biomass C stock and the ratios of above- to below-ground biomass are more likely an artifact of methodologies and allometric equations used, rather than actual differences in mangrove structure.

The Zambezi River Delta mangrove system affirms the consistency of the large C stocks that are characteristic of mangroves across a relatively large and hydrologically diverse area. However, the distribution of the C stock magnitude varies spatially throughout any study area. This spatial heterogeneity can be due to variability in any one or more of the potential C pools. The spatial variability in the Zambezi River Delta was driven by differences in overstory biomass, due to variation of forest structure and composition which can be influenced by tidal range, nutrient availability, and geomorphology (Bouillon et al., 2008; Alongi, 2014). In contrast to our study, soil C can sometimes drive differences in spatial variation of C stocks, as was the case in the Dominican Republic, where soil C means ranged from 546 Mg ha^{-1} to 1084 Mg ha^{-1} depending on vegetation type (Kauffman et al., 2014).

5.4. Inventory approach

Unbiased inventories that provide a basis for quantifying uncertainties and which can be used as the foundation for MRV are fundamental to REDD+ and similar programs. Our stratified random sampling design, implemented with the SDSS, was effective and efficient in inventorying the vast and remote Zambezi River Delta. Stratification can produce estimates with increased precision compared with simple random sampling, especially when the variable used to define the strata is highly correlated with the outcome being measured (U.S. EPA, 2002), as is the case with canopy height (stratification variable) and biomass (measured variable). Accordingly, other bases for stratification could include metrics such as cover type, canopy density, and geomorphic position (Kauffman and Donato, 2012; Howard et al., 2014; Jones et al., 2014). The advantage of the canopy height dataset as a stratification variable is that it is available for the entire African coast, and the functional relationship of canopy height to stand biomass is established (Simard et al., 2011; Fatoyinbo and Simard, 2013). The stratification variable does not bias the calculated biomass, which is dependent on tree diameter. Instead, the canopy height strata reflect a common attribute as a means to classify the inventory area.

Our approach illustrates the efficacy of using inventory methodologies, as well as the level of precision that can be attained. The UN REDD+ program has specific guidance regarding acceptable levels of uncertainty and asks for the precision of a 95% confidence interval to be equal to or less than 15% of the recorded estimate (VCS, 2012). Our sampling design allowed us to achieve a precision of a 95% confidence interval equal to 6% of our ecosystem C stock estimate, well within the REDD+ guidelines.

These plots could be used for monitoring in several different ways, depending on the time horizon and available resources. For instance, a complete inventory could be performed at five-year intervals which should yield precision levels similar to that achieved in this study. An alternative is to perform a rotating panel design where a different fifth of the plots are sampled every year, resulting in a complete inventory of all plots after five years. Such an approach allows for annual updates to identify important conditions occurring on the plots and spreads the resources evenly over the five years. If resources are very limited, a subsample of the plots may be sampled after five years which would result in no annual information and less precision.

6. Conclusion

This project was the first operational-scale, comprehensive mangrove forest inventory in East Africa. We employed a stratified random sampling design, based on existing and publically accessible remote-sensing data, as the basis for quantifying C stocks. This approach resulted in very precise estimates, with uncertainties falling well-within international guidelines, thus demonstrating the importance of well-designed assessments. The results of this study will not only be included in a national forest inventory being conducted by the government of Mozambique, but will also provide the foundation for a new Blue Forest project that is being implemented by WWF-Mozambique with funding by the Global Environmental Facility. The project's main goal is to advance a REDD+ scheme through the production of a Project Design Document (PDD) for C finance application in the Zambezi delta applicable to an area covering a total of 25,000 ha.

Acknowledgments

This work was made possible by US AID support to the USFS under the US AID Mozambique Global Climate Change Sustainable Landscape Program, in collaboration with the Natural Resource Assessment Department of the Government of Mozambique. Denise Nicolau, Itelvino Cunat, and Rito Mabunda provided invaluable logistical support during the planning and implementation of field missions. Célia Macamo and Salamão

Bandeira assisted prior to, and during field work, with identification of mangrove and other plant species. The staff of the Soils Lab at Universidade de Eduardo Mondlane processed the soil and biomass samples. Julie Arnold and Artheera Bayles at the USFS Center for Forested Wetlands Research assisted with soil C analyses. The success of this project would not have been possible without the hard work and dedication of the 2012 and 2013 mission field crews. We also thank Matthew Warren and Randall Kolka for their thorough and helpful reviews of an earlier manuscript draft.

References

Adame, M.F., Kauffman, J.B., Medina, I., Gamboa, J.N., Torres, O., Caamal, J.P., Reza, M., Herrera-Silveira, J.A., 2013. Carbon stocks of tropical coastal wetlands within the karstic landscape of the Mexican caribbean. PLoS One 8, e56569.

Alongi, D.M., 2002. Present state and future of the world's mangrove forests. Environ. Conservation 29, 331–349.

Alongi, D.M., 2012. Carbon sequestration in mangrove forests. Carbon Manage. 3, 313–322.

Alongi, D.M., 2014. Carbon cycling and storage in mangrove forests. Annu. Rev. Mar. Sci. 6, 195–219.

Barbosa, F.M.A., Cuambe, C.C., Bandeira, S.O., 2001. Status and distribution of mangroves in Mozambique. S. Afr. J. Bot. 67, 393–398.

Bartlett, J.E., Kotrlik, J.W., Higgins, C.C., 2001. Organizational research: determining appropriate sample size in survey research. Inf. Technol., Learning, Perfomance J. 19, 43–50.

Bechtold, W.A., Patterson, P.L., 2005. The enhanced forest inventory and analysis program-national sampling design and estimation procedures. In: General Technical Report. U.S. Department of Agriculture, Forest Service, Southern Research Station, Asheville, North Carolina USA, p. 85.

Beilfuss, R.D., Moore, D., Bento, C., Dutton, P., 2001. Patterns of vegetation change in the Zambezi Delta, Mozambique. In: Program for the Sustainable Management of Cahora Bassa Dam and the Lower Zambezi Valley.

Beilfuss, R.D., Santos, D.D., 2001. Patterns of hydrological change in the Zambezi Delta, Mozambique. In: Program for the Sustainable Management of Cahora Bassa Dam and the Lower Zambezi Valley.

Bento, C.M., Beilfuss, R.D., Hockey, P.A., 2007. Distribution, structure and simulation modelling of the Wattled Crane population in the Marromeu Complex of the Zambezi Delta, Mozambique. Ostrich-J. Afr. Ornithol. 78, 185–193.

Bouillon, S., Borges, A.V., Castañeda-Moya, E., Diele, K., Dittmar, T., Duke, N.C., Kristensen, E., Lee, S.Y., Marchand, C., Middleburg, J.J., Rivera-Monroy, V.H., Smith, T.J.I., Twilley, R.R., 2008. Mangrove production and carbon sinks: a revision of global budget estimates. Global Biogeochem. Cycles 22, GB2013.

Brown, J.K., 1971. A planar intersect method for sampling fuel volume and surface area. Forest Sci. 17, 96–102.

Chmura, G.L., Anisfeld, S.C., Cahoon, D.R., Lynch, J.C., 2003. Global carbon sequestration in tidal, saline wetland soils. Global Biogeochem. Cycles, 17.

Cochran, W.G., 1977. Sampling Techniques. John Wiley, New York.

Cohen, R., Kaino, J., Okello, J.A., Bosire, J.O., Kairo, J.G., Huxam, M., Mencuccini, M., 2013. Propagating uncertainty to estimates of above-ground biomass for Kenyan mangroves: a scaling procedure from tree to landscape level. Forest Ecol. Manage. 310, 968–982.

Coleman, J., 2004. The Zambezi Delta. In: The World Delta Database. Louisiana State University, <www.geol.lsu.edu/WDD/AFRICAN/Zambezi>.

Cormack, R., 1988. Statistical challenges in the environmental sciencesL a personal view. J. R. Stat. Soc. Ser. A (Stat. Soc.), 201–210.

Davies, B.R., Beilfuss, R.D., Thoms, M.C., 2000. Cahora Bassa retrospective, 1974–1997: effects of flow regulation on the Lower Zambezi River. Verhandlungen des Internationalen Verein Limnologie 27, 1–9.

Densham, P.J., 1991. Spatial decision support systems. In: Maguire, D.J., M.G., Rhind, D.W. (Eds.), Geographical Information Systems: Principles and Applications. John Wiley and Sons, New York, pp. 403–412.

Dittmar, T., Hertkorn, N., Kattner, G., Lara, R.J., 2006. Mangroves, a major source of dissolved organic carbon to the oceans. Global Biogeochem. Cycles 20, GB1012.

Donato, D.C., Kauffman, J.B., Mackenzie, R.A., Ainsworth, A., Pfleeger, A.Z., 2012. Whole-island carbon stocks in the tropical Pacific: implications for mangrove conservation and upland restoration. J. Environ. Manage. 97, 89–96.

Donato, D.C., Kauffman, J.B., Murdiyarso, D., Kurnianto, S., Stidham, M., Kanninen, M., 2011. Mangroves amongst the most carbon-rich forests in the tropics. Nat. Geosci. 4, 293–297.

Fatoyinbo, T.E., Simard, M., 2013. Height and biomass of mangroves in Africa from ICESat/GLAS and SRTM. Int. J. Remote Sens. 34, 668–681.

Fromard, F., Puig, H., Mougin, E., Marty, G., Betoulle, J.L., Cadamuro, L., 1998. Structure, above-ground biomass and dynamics of mangrove ecosystems: new data from French Guiana. Oecologia 115, 39–53.

Giri, C., Ochieng, E., Tieszen, L.L., Zhu, Z., Singh, A., Loveland, T., Masek, J., Duke, N., 2011. Status and distribution of mangrove forest of the world using earth observation satellite data. Global Ecol. Biogeography 20, 154–159.

Government of Mozambique. 2009. National Report on Implementation of the Convention on Biological Diversity in Mozambique. Maputo, Mozambique.

Gullison, R.E., Frumhoff, P.C., Canadell, J.G., Field, C.B., Nepstad, D.C., Hayhoe, K., Avissar, R., Curran, L.M., Friedlingstein, P., Jones, C.D., Nobre, C., 2007. Tropical forests and climate policy. Science 316, 985–986.

Hoguane, A.M., 2007. Perfil Diagnóstico da Zona Costeira de Moçambique. Revista de Gestão Costeira Integrada 7, 69–82.

Howard, J., Hoyt, S., Isensee, K., Pidgeon, E., Telszewski, M., 2014. Coastal blue carbon: methods for assessing carbon stocks and emissions factors in mangroves, tidal salt marshes, and sea grass meadows. In: Conservation International, Intergovernmental Oceanographic Commission of UNESCO. International Union for Conservation of Nature, Arlington, Virgina, USA.

IPCC, 2013. The physical science basis. Contribution of working group I to the fifth assessment report of the intergovernmental panel on climate change. Cambridge University Press, United Kingdom and New York, NY, USA, p. 1535.

Janzen, D.H., 1985. Mangroves: where's the understory? J. Tropical Ecol. 1, 89–92.

Jones, T.G., Ratsimba, H.R., Ravaoarinorotsihoarana, L., Cripps, G., Bey, A., 2014. Ecological variability and carbon stock estimates of mangrove ecosystems in Northwestern Madagascar. Forests 5, 177–205.

Kauffman, J.B., Donato, D.C., 2012. Protocols for the measurement, monitoring and reporting of structure, biomass and carbon stocks in mangrove forests. In: Center for International Forestry Research, Bogor, Indonesia.

Kauffman, J.B., Heider, C., Cole, T.G., Dwire, K.A., Donato, D.C., 2011. Ecosystem carbon stocks of micronesian mangrove forests. Wetlands 31, 343–352.

Kauffman, J.B., Heider, C., Norfolk, J., Payton, F., 2014. Carbon stocks of intact mangroves and carbon emissions arising from their conversion in the Dominican Republic. Ecol. Appl. 24, 518–527.

Kirui, B.K., 2006. Allometric Relations for Estimating Aboveground Biomass of Naturally Growing Mangroves, *Avicennia marina* Forsk (Vierh). and *Rhizophora mucronata* Lam. along the Kenya Coast. Egerton University.

Komiyama, A., Havanond, S., Srisawatt, W., Mochida, Y., Fujimoto, K., Ohnishi, T., Ishihara, S., Miyagi, Y., 2000. Top/root biomass ratio of a secondary mangrove (*Ceriops tagal* (Perr.) C.B. Rob.) forest. Forest Ecol. Manage. 139, 127–134.

Komiyama, A., Ogino, K., Aksornkoae, S., Sabhasri, S., 1987. Root biomass of a mangrove forest in Southern Thailand. 1. Estimation by the trench method and the zonal structure of root biomass. J. Tropical Ecol. 3, 97–108.

Komiyama, A., Ong, J.E., Poungparn, S., 2008. Allometry, biomass, and productivity of mangrove forests: a review. Aquat. Bot. 89, 128–137.

Komiyama, A., Poungparn, S., Kato, S., 2005. Common allometric equations for estimating the tree weight of mangroves. J. Tropical Ecol. 21, 471–477.

Kristensen, E., Bouillon, S., Dittmar, T., Marchand, C., 2008. Organic carbon dynamics in mangrove ecosystems: a review. Aquat. Bot. 89, 201–219.

Nusser, S., Breidt, F., Fuller, W., 1998. Design and estimation for investigating the dynamics of natural resources. Ecol. Appl. 8, 234–245.

Elmer, Perkin, 2010. Organic Elemental Analysis of Soils-Understanding the Carbon-Nitrogen Ratio. Perkin Elmer, Waltham, MA, USA.

Rahman, M.M., Khan, M.N.I., Hoque, A.K.F., Ahmed, I., 2014. Carbon stock in the Sundarbans mangrove forest: spatial variations in vegetation types and salinity zones. Wetlands Ecol. Manage.

SAS Inc., 2011. SAS/STAT 9.3 User's Guide. SAS Institute Inc., Cary, North Carolina.

Simard, M., Pinto, N., Fisher, J.B., Baccini, A., 2011. Mapping forest canopy height globally with spaceborne lidar. J. Geophys. Res. 116, G04021.

Slim, F.J., Gwada, P.M., Kodjo, M., Hemminga, M.A., 1996. Biomass and litterfall of *Ceriops tagal* and *Rhizophora mucronata* in the Mangrove Forest of Gazi Bay, Kenya. Mar. Freshwater Res. 47, 999–1007.

Thomas, G.W., 1996. Soil pH and soil acidity. In: Methods of Soil Analysis: Part 3-Chemical Methods. Soil Science Society of America, Madison, Wisconsin, pp. 475–490.

Tweddle, D., 2013. Lower Zambezi. In: Freshwater Ecoregions of the World <feow.org/ecoregions/details/lower_Zambezi>.

UN-REDD, 2011. The UN-REDD programme strategy 2011–2015. In: United Nations Collaborative Initiative on Reducing Emissions from Deforestation and Forest Degradation (REDD+) in Developing Countries.

U.S. EPA, 2002. Guidance for choosing a sampling design for environmental data collection (EPA QA/G-5S).

van der Werf, G.R., Morton, D.C., DeFries, R.S., Olivier, J.G.J., Kasibhatla, P.S., Jackson, R.B., Collatz, G.J., Randerderson, J.T., 2009. CO_2 emissions from forest loss. Nat. Geosci. 2, 737–738.

Van Wagner, C.E., 1968. The line intersect method in forest fuel sampling. Forest Sci. 14, 20–26.

VCS, 2012. REDD methodological module: estimation of uncertainty for REDD project activities (X-UNC). TerraCarbon, Verified Carbon Standard.

Vilankulos, M., Marquez, M.R., 2000. Physical characterization of the coastal zone of mangrove areas in the districts of Dondo and Marromeu, Sofala, based on interpretation of aerial photographs. In: Doddema, M. (Ed.), Baseline Data and Evaluation Procedures for the Formulation of Mangrove Resources Management Plan in the Northern Part of Sofala Province. Direcçao Nacional de Florestas e Fauna Bravia, Maputo.

Wang, G., Guan, D., Peart, M.R., Chen, Y., Peng, Y., 2013. Ecosystem carbon stocks of mangrove forest in Yingluo Bay, Guangdong Province of South China. Forest Ecol. Manage. 310, 539–546.

World Agroforestry Database. 2013. Wood density database <http://worldagroforestry.org/regions/southeast_asia/resources/wood-density-database>.